



The Mechanism of H₂S Poisoning Ni/YSZ Electrode Studied by Impedance Spectroscopy

Ting Shuai Li and Wei Guo Wang^{*,z}

Division of Fuel Cell and Energy Technology, Ningbo Institute of Material Technology and Engineering,
Chinese Academy of Sciences, Ningbo 315201, China

The two specific processes of hydrogen sulfide poisoning a solid oxide fuel cell (SOFC) were studied by impedance spectroscopy in galvanostatic mode at 800 °C. The polarization resistance increased by exposure to H₂S within 30 min and then remained nearly stable in the subsequent aging test, accounting for an abrupt cell performance drop. A successive sluggish degradation was corresponding to the slow increase of the series resistance, which can be attributed to the contaminated nickel catalyst at the yttria-stabilized zirconia (Ni/YSZ) anode supported layer. The results indicated the establishment of a two-step mechanism of H₂S poisoning an SOFC.

© 2010 The Electrochemical Society. [DOI: 10.1149/1.3526134] All rights reserved.

Manuscript submitted October 23, 2010; revised manuscript received November 17, 2010. Published December 16, 2010.

The H₂S poisoning is an important issue for solid oxide fuel cells (SOFCs) at various operational conditions. The relative mechanisms have been paid much attention in previous studies.¹⁻⁵ Zha et al.¹ attributed the initial sharp performance degradation to rapid adsorption of sulfur onto the nickel surface and the subsequent slow degradation to some processes related to the reconstruction of nickel. The surface-adsorbed sulfur would react with nickel to form nickel sulfide including Ni₃S₂ (Ref. 2 and 4) and Ni₇S₆ with a small amount of Ni₃S₂.⁵ Wang and Liu also predicted a new S-Ni phase by a computational study.⁶ Another possible exploration could be the changes of the anode structure due to the melting of nickel sulfides.^{7,8} It can be confirmed that the rapid adsorption of sulfur onto the nickel surface and the reaction of nickel and sulfur are the key to understand the initial sharp degradation. However, the successive long-term slow degradation is still not well understood.

In the present study, the two different processes of H₂S poisoning an SOFC are identified using an impedance spectroscopy technique. The first stage of acute deterioration is further confirmed based on our previous study⁹ and a new mechanism for the second period of sluggish degradation is concurrently proposed, which may be helpful in reducing the H₂S poisoning degree only by selecting a more highly efficient catalyst in the anode active layer instead of substituting the entire body of the anode material.

Experimental

The cells used for the test in this study are typical anode supported planar fuel cells manufactured at NIMTE. The cell has an 8YSZ (yttria-stabilized zirconia) electrolyte and an La_{1-x}Sr_xMnO₃/YSZ cathode. Details on composition of the electrodes etc. are given elsewhere.¹⁰ The as-fabricated cell has an active area of 10 cm × 10 cm, and it was cut into samples of 5 cm × 5.8 cm that had active areas of 4 cm × 4 cm for the tests. The setup for cell testing has been described elsewhere.¹¹

The cells were first galvanostatically operated at 0.50 A cm⁻² at 800 °C for 50 h to reach a stable state with 0.5 standard-state liter per minute (SLM) H₂ as fuel and 2 SLM air as cathode gas. Impedance spectra were acquired at every 15 min after 0.2% H₂S injection at 0.25 and 0.50 A cm⁻² with an IM6ex (ZAHNER, Germany) electrochemical station using a four-point measurement method. The perturbation voltage was set at an amplitude of and the scanning frequency ranged from 1 MHz to 0.05 Hz. The poisoned sample was analyzed after electrochemical measurement using a Hitachi S4800 (Hitachi, Japan) field emission scanning electron microscope/energy dispersive spectroscopy (FE-SEM/EDS).

Results and Discussion

Figure 1 shows the impedance spectra measured at 0.25 and 0.50 A cm⁻² when the cells are exposed to 0.2% H₂S at 800 °C. The variation of the impedance spectra is representative of the effect of H₂S contaminant on the anodic processes because the cathode is always exposed to the same environment. The polarization resis-

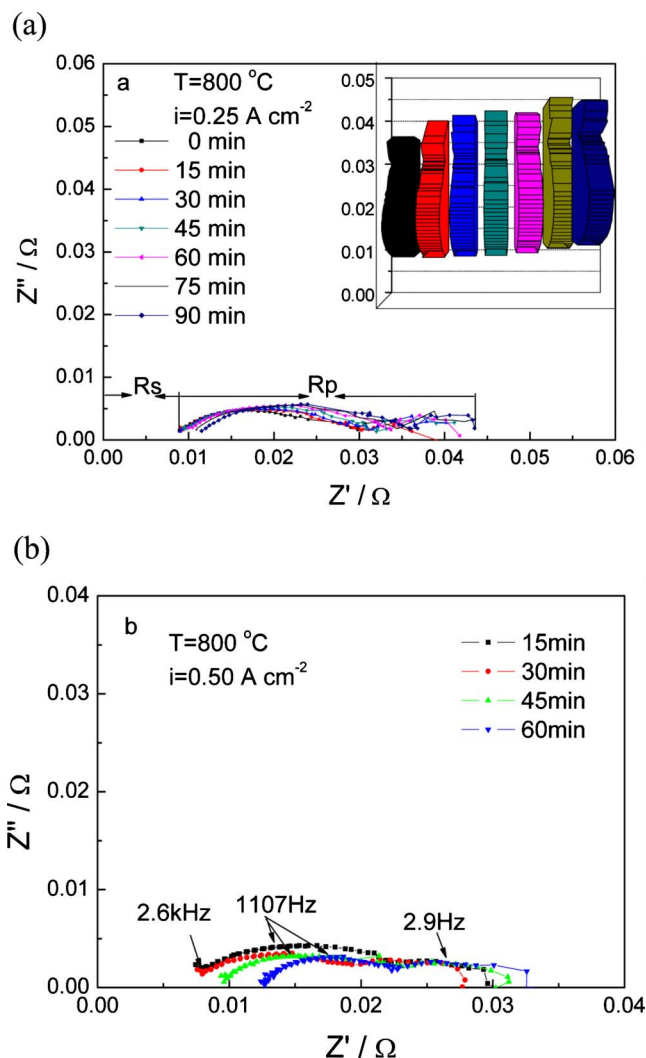


Figure 1. (Color online) The variation of EIS recorded at 800 °C with application of (a) 0.25 A cm⁻² and (b) 0.5 A cm⁻².

* Electrochemical Society Active Member.

^z E-mail: wgwang@nimte.ac.cn

Table I. The specific values of Rs and Rp obtained at various poisoning times.

$i/A\text{ cm}^{-2}$	R/m Ω	0 min ^a	15 min	30 min	45 min	60 min	75 min	90 min
0.25	Rs	8.9	9.0	9.0	9.5	10.0	11.0	11.5
0.25	Rp	27.0	31.4	31.2	32.3	31.8	31.3	32.0
0.50	Rs		8.0	8.0	9.6	12.7		
0.50	Rp		19.7	21.6	21.6	20.2		

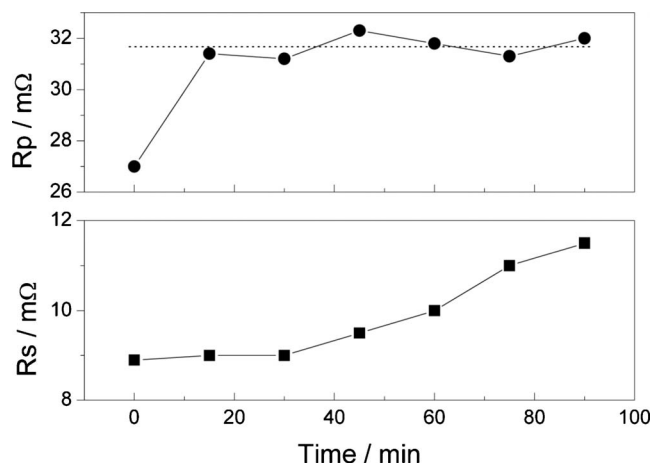
^a Before poisoning test.

tance (Rp) seems to be more stable at 0.50 A cm⁻² and the series resistance (Rs) explicitly increases with time cause at both 0.25 and 0.50 A cm⁻² upon the injection of H₂S at a fixed period. The specific values of Rs and Rp have been summarized in Table I. Rs is the sum of the electrolyte resistance, the electrode material resistance of both the anode and the cathode, and the contact resistance between the electrodes and current collectors.¹² The material resistance can theoretically remain constant at the identical temperature when no phase transformation occurs. Rp mainly originates specific processes including mass transport and electrochemical reaction at the anode and cathode sides (electrode response, diffusion/conversion).¹³

Sulfur depositing onto the surface of nickel results in the loss of active sites at the anodic functional layer, which can immediately deteriorate electrochemical reactions occurring at the triple phase boundary. These processes are corresponding to the gas diffusion and conversion at the anode side, and the observed variations are mainly reflected by the low frequencies of the related impedance spectra. The increase of ohmic resistance of an SOFC is completely associated with the processes in accordance with the highest frequencies, as indicated in Fig. 1a.¹⁴

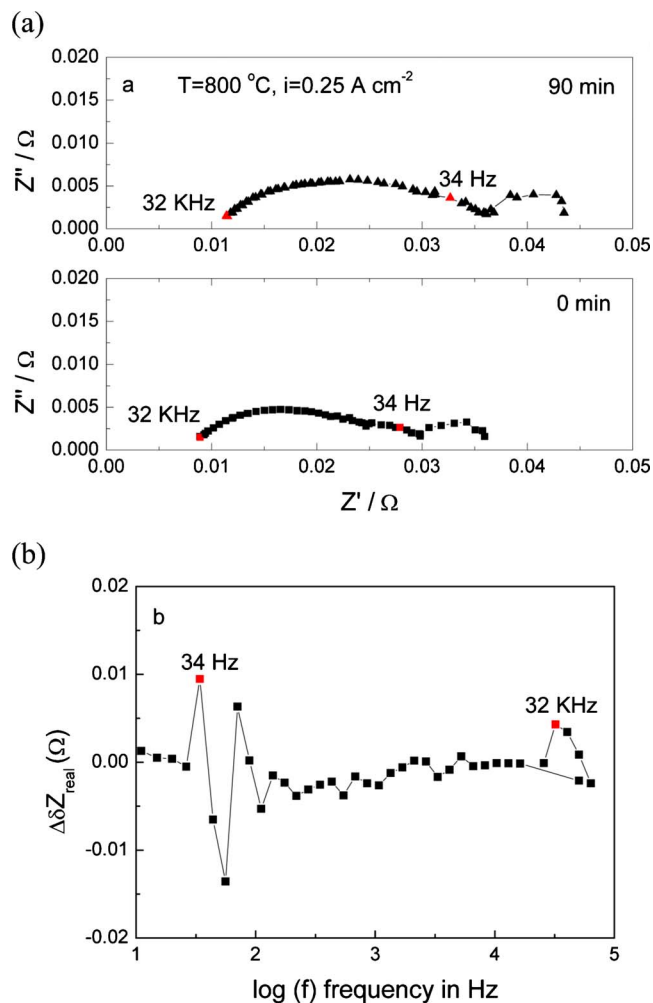
Figure 2 demonstrates the variation of Rs and Rp with time cause when the cell is galvanostatically operated at 0.25 A cm⁻² by the exposure to H₂S for 90 min. A sharp increase in the Rp value is measured within 20 min, which is corresponding to the initial performance drop. Our previous study indicated that sulfur mainly attacked the nickel catalyst at an anodic active zone by a short term exposure of H₂S,⁹ which thus supported this conclusion that the initial rapid degradation can be attributed to sulfur adsorption on the nickel surface and the formation of nickel sulfide at the anode active layer. Conversely, the series resistance first remains constant and then increases with the elapsing time cause, which may reflect the mechanism of the sequential sluggish degradation.

Figure 3a gives the specific data of impedance spectra measured upon the exposure to H₂S for 0 min (before poisoning) and 90 min. The difference between the derivatives of the two spectra $\Delta\delta Z_{\text{real}}$

**Figure 2.** The changes of Rs and Rp vs elapsing time cause measured at 0.25 A cm⁻².

$= [\delta Z_{\text{real}}^{\text{time1}} - \delta Z_{\text{real}}^{\text{time2}}] / \log f$ is plotted versus $\log f$ in Fig. 3b, which is used to highlight where the two spectra deviate.¹⁵ In the difference plot, two peaks at 32 kHz and 34 Hz are clear. The change of the low frequency region (34 Hz) is related to gas diffusion at Ni/YSZ cermet anodes.¹⁶ The key to understand this process is that the loss of active sites at the anodic zone is due to the immediate H₂S poisoning of the nickel catalyst, resulting in the increase of difficulty in gas diffusing to the triple phase boundary to complete the electrochemical reaction. The deviation occurring at 34 kHz can be corresponding to the subsequent slight increase of the series resistance.

A cross section microstructure of the anode poisoned at 0.25 and 0.50 A cm⁻² has been analyzed as shown in Fig. 4a and 4b. The

**Figure 3.** (Color online) (a) The specific data of EIS tested at 0.25 A cm⁻² before H₂S injection and after injecting H₂S for 90 min. (b) Difference plot $\Delta\delta Z_{\text{real}} = [\delta Z_{\text{real}}^{\text{time1}} - \delta Z_{\text{real}}^{\text{time2}}] / \log f$ vs $\log f$ obtained from the data shown in (a).

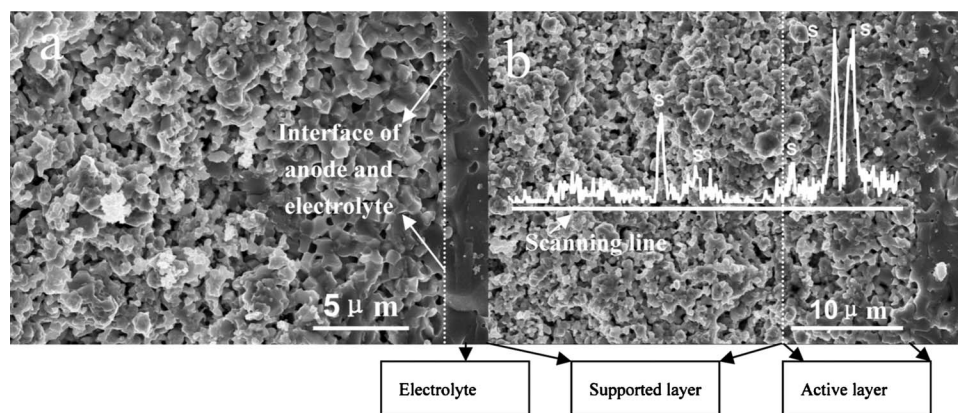


Figure 4. (a) Microstructure of the cell anode after being poisoned at 0.25 A cm^{-2} . (b) Sulfur distribution at the anodic layer detected by EDS using the line scanning mode.

interface of the anode and the electrolyte is not destroyed after the poisoning test, because there are no observable agglomeration and crack and delamination from SEM pictures. Conversely, the sulfur may mainly attack the catalyst nickel and hardly contaminate the YSZ electrolyte.⁹ Therefore, the increase of R_s can be finally attributed to conductive decrease of the anode part. The result of EDS analysis, as shown in Fig. 4b, indicates that the sulfur poisoning area extends to the anode supported layer, which can reduce the conductivity of nickel when nickel sulfide is formed.

Conclusions

The specific processes of H_2S poisoning an SOFC have been identified by impedance spectroscopy. The initial sharp performance drop is corresponding to the adsorption of sulfur onto the nickel surface at the anode active layer and the formation of nickel sulfides. The subsequent sluggish degradation may be related to the decomposition of H_2S at the anode supported region, resulting in a decrease of conductivity. The two-step degradation is confirmed by material analysis after the poisoning test.

Acknowledgments

This work was conducted at Ningbo Institute of Material Technology and Engineering, Chinese Academy of Sciences and was financially supported by the National 863 Program (no. 2007AA05Z140 and no. 2009AA05Z122). Colleagues at Division of Fuel Cell and Energy Technology are acknowledged for their assistance in the single cell manufacture.

Chinese Academy of Sciences assisted in meeting the publication costs of this article.

References

1. S. Zha, Z. Cheng, and M. Liu, *J. Electrochem. Soc.*, **154**, B201 (2007).
2. K. Sasaki, K. Susukif, A. Iyoshi, M. Uchimura, N. Imamura, H. Kusaba, Y. Teraoka, H. Fuchino, D. K. Tsujimoto, Y. Uchida, et al., *J. Electrochem. Soc.*, **153**, A2023 (2006).
3. P. Lohsoontorn, D. J. L. Brett, and N. P. Brandon, *J. Power Sources*, **183**, 232 (2008).
4. Z. Cheng and M. Liu, *Solid State Ionics*, **178**, 925 (2007).
5. J. Dong, Z. Cheng, S. Zha, and M. Liu, *J. Power Sources*, **156**, 461 (2006).
6. J. H. Wang and M. Liu, *Electrochem. Commun.*, **9**, 2212 (2007).
7. A. Ishikura, S. Sakuno, N. Komiyama, H. Sasatsu, N. Masuyama, H. Itoh, and K. Yasumoto, *ECS Trans.*, **7**(1), 845 (2007).
8. A. Lussier, S. Sofie, J. Dvorak, and Y. U. Idzerda, *Int. J. Hydrogen Energy*, **33**, 3945 (2008).
9. T. S. Li, W. G. Wang, T. Chen, H. Miao, and C. Xu, *J. Power Sources*, **195**, 7025 (2010).
10. T. S. Li, W. G. Wang, H. Miao, T. Chen, and C. Xu, *J. Alloys Compd.*, **495**, 138 (2010).
11. T. S. Li, H. Miao, T. Chen, W. G. Wang, and C. Xu, *J. Electrochem. Soc.*, **156**, B1383 (2009).
12. T. Kato, K. Nozaki, A. Negishi, K. Kato, A. Monma, Y. Kaga, S. Nagata, K. Takano, T. Inagaki, H. Yoshida, et al., *J. Power Sources*, **133**, 169 (2004).
13. R. Barfod, A. Hagen, S. Ramousse, P. V. Hendriksen, and M. Mogensen, *Fuel Cells*, **6**, 141 (2006).
14. Q. A. Huang, Rob Hui, B. Wang, and J. Zhang, *Electrochim. Acta*, **52**, 8144 (2007).
15. R. Barfod, M. Mogensen, T. Klemensø, A. Hagen, Y. L. Liu, and P. V. Hendriksen, *J. Electrochem. Soc.*, **154**, B371 (2007).
16. S. Primdahl and M. Mogensen, *J. Electrochem. Soc.*, **146**, 2827 (1999).